Extrapolation of Asymmetry Data to Determine A_o

Marcy L. Stutzman, Timothy J. Gay,

A. Extrapolation Functions

The ultimate goal of a Mott asymmetry measurement is to provide an absolute value of the incident electron polarization, P_e. This is obtained by knowing the theoretical Sherman function S: $P_e = A_o/S$. Since S is calculated, as shown in section xxx, assuming elastic single-collision conditions, A_o corresponds to the Mott asymmetry for the same conditions. In principle, this requires that elastic scattering be guaranteed by energy filtering, and that a vanishingly thin target be used to eliminate the possibility of plural scattering. In practice one extrapolates measured asymmetries to zero target thickness, while providing the best possible energy discrimination against inelastically-scattered electrons [1]. At incident electron energies below ~200 keV, "retarding field" Mott polarimeters allow the precise extrapolation of asymmetries to zero energy loss in conjunction with target thickness extrapolations [2]. (Energy extrapolation alone is not sufficient to guarantee single-scattering conditions; see reference [3], Figure 9.) At MeV energies such as ours, where semiconductor or scintillator-based electron detection is used, energy discrimination becomes more difficult and a target thickness extrapolation must be employed to determine A_o. Described here is the target thickness extrapolation techniques used to determine A_o from a series of asymmetry measurements from finite thickness foils.

In our experiment, we measured Mott asymmetries, $A(t)$, as a function of Au target foil thickness, t, ranging from 0.050 μm to 1μm. At 5 MeV in this foil thickness range, $A(t)$ is a monotonically decreasing function of t, losing about 20% of its value as t increases from 0 μm (A_o) to 1 μm. The function $A(t)$ has a weak curvature with a positive second derivative. Historically, and because of the lack of any compelling theoretical guidance, a variety of functional forms have been used to fit $A(t)$, and thus determine A_o [3,4, 4.1,4.2,4.3]. These have all been of the form

$$A^q(t) = A_o(1 - at), \qquad\qquad\qquad (i)$$

$$A(t) = A_o \frac{(1-at)}{(1+bt)}, \tag{ii}$$

or $$A(t) = a + be^{-ct}, \tag{iii}$$

where q = 1, -1, or -2, and a, b, c, and A_o are fitting parameters. In form (iii), $a+b = A_o$ or, if b is set to zero, $A_o = a$.

As we will see below, the precision with which A_o can be determined is limited primarily by the uncertainty in the target thicknesses. These uncertainties are typically 5-8% of the t values themselves. An attractive alternative to thickness extrapolations is to consider A vs. the count rate summed from both detectors, $R(t)$. Uncertainties in the count rates are due mostly drift between stability runs, believed to be due to instability in the measured beam current, to which the rates must be normalized. These uncertainties are typically much smaller on a percentage basis than the uncertainties in t. In this work, we will thus also consider R -dependent extrapolation functions.

The GEANT4 simulations discussed in Section X.X give us some confidence that a fitting form of type (ii) is the most appropriate function with which to extrapolate our $A(t)$ data to A_o. Having said this, we prefer a more conservative approach espoused in reference [4]. In that work, the $A(t)$ data were fit to four functions of types (i) and (ii). It was shown that the spread in the (correlated) fit values of A_o was somewhat larger than the statistical uncertainty in the A_o values given by a specific fitting form. As a result, the uncertainty in the weighted mean of the four intercepts (their quoted final value of A_o) was assigned to be such that $\pm 2\sigma$ error bars encompassed all four intercepts.

To this end, we have applied a more general procedure to assess the precision of our final A_o values. Our $A(t)$ data were fit using the method of Padé approximates [5]. Padé approximates (PAs) are a class of rational fractions which are typically well-behaved and converge more rapidly than Taylor series approximations to a set of data for extrapolation. The PAs, $A_{n,m}$, take the form

$$A_{n,m}(t) = \frac{P_m(t)}{Q_n(t)} = \frac{A_0(a_n t^n + a_{n-1} t^{n-1} + \cdots + a_2 t^2 + a_1 t + a_0)}{(b_m t^m + b_{m-1} t^{m-1} + \cdots + b_2 t^2 + b_1 t + b_0)} \tag{iv}$$

for $m \geq 0$ and $n \geq 1$. The form of Eq. (i) thus corresponds to a $A_{1,0}$ PA for $q = 1$, an $A_{0,1}$ for $q = -1$, and an $A_{0,2}$ PA for $q = -2$; equations (ii) corresponds to a PA of $A_{1,1}$. Finally, equation (iii) is essentially a PA of arbitrarily high order s of the form $A_{s,0}$.

We began our analysis by using the $A_{1,0}$ form to fit a given $A(t)$ data set, and then increase both n and m until application of an F test indicates that higher orders of n and/or m are not justified [6]. As we will show below, the only PA forms that were not excluded using F-tests for the $A(t)$ data were the $A_{1,0}$, $A_{0,1}$, $A_{1,1}$, and $A_{2,0}$ forms. All fits that passed the F-test were then also subjected to a reduced chi-squared analysis as well [6], which for the $A(t)$ data suggests that the $A_{1,0}$ can also be removed from the set of fits used to extrapolate the data to find A(0). Tables 1 and 2 show the results of the PA analysis for the A(t) data for runs 1 and 2, with both runs yielding the same allowed forms of $A_{0,1}$, $A_{1,1}$, and $A_{2,0}$.

Table 1 shows the results of the Pade analysis for the fits of the A(t) data for Run 1 (top) and Run 2 (bottom) to the various forms $A_{n,m}$. For each PA, the intercept(with uncertainty), the F-test result and the reduced $\chi 2$ value are shown. Forms in red are excluded by the F-test, in blue are excluded using the the reduced $\chi 2$ value. PAs that will be considered are shown in bold type.

A(t),**Run1** Pade(n,m)	(0,m)	(1,m)	(2,m)	(3,m)
(n,0)		43.82(15),n/a,2.2	**44.04(14),7.5,1.2**	44.25(18),2.8,0.97
(n,1)	**44.03(11),8.0,1.2**	**44.09(14),6.3,1.8**	44.35(38),-2.2,5.4	
(n,2)	44.09(14),0.3,1.5	43.98(33),-0.41,2.5		

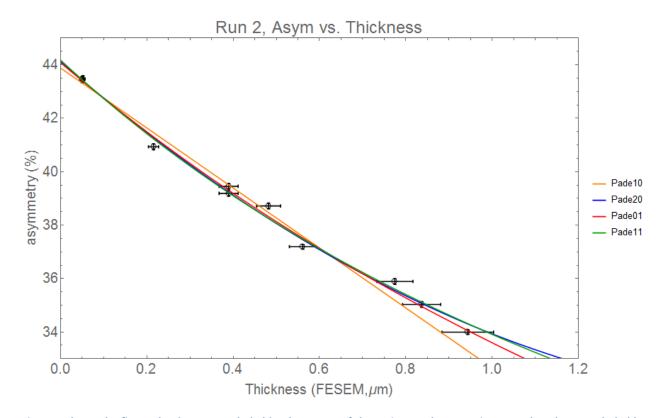| A(t),**Run2** Pade(n,m)	(0,m)	(1,m)	(2,m)	(3,m)
(n,0)		43.84(16),n/a,2.7	**44.12(14),10,1.3**	44.35(17),3.4,0.96
(n,1)	**44.08(11),9.4,1.3**	**44.18(15),8.5,1.6**	44.45(39),-2.0,4.6	
(n,2)	44.17(15),0.8,1.36	44.14(65),-0.04,2.0		

Figure 1 shows the fits to the data not excluded by the F-tests of the various Pade Approximants. Though not excluded by the F-tests, the Pade10 form will be eliminated from the functions used to determine the intercept A(0) due to its poor fit to the data, as shown by the reduced χ2 value of 2.7.

As mentioned previously, further reduction of the allowed fits to the data can be made using other methods. For example, the $A_{1,0}$ fit to the $A(t)$ data appears to fit the data poorly, and the reduced χ2 value of 2.7 indicates that this is unlikely to be a good fit to the data (with a 1.5% chance of exceeding χ2, Bevington table C-4). Figure 4 shows the summary of the intercepts for runs 1 and 2 as determined from the A(t) data.

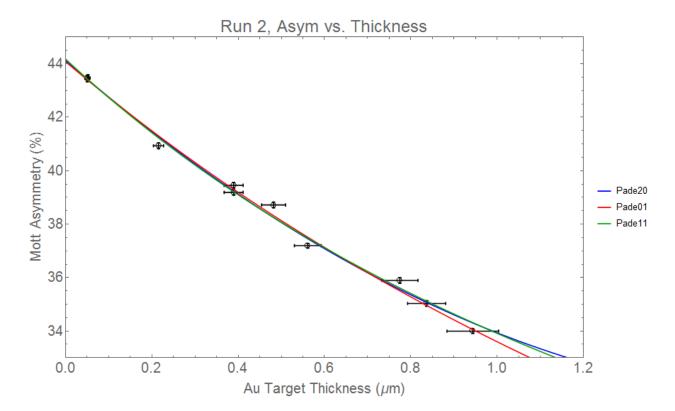Figures 2 and 3 show the allowed fits and fit parameters for A(t) for Run 1 and Run 2

Run 2, Asym vs. Thickness

Pade20
Pade01
Pade11

Figure 2

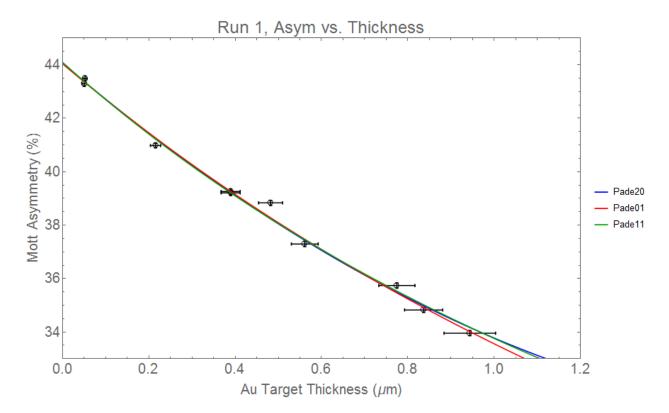| Fit, A(t) Run2	Parameters	Reduced χ2
Pade01	$\dfrac{44.08(11)}{1 + 0.31(01)x}$	1.15
Pade20	$44.12(15) - 14.0(10)x + 3.8(1.2)x^2$	1.29
Pade11	$\dfrac{44.18(15) + 5.6(5.8)x}{1 + 0.47(16)x}$	1.18

Figure 3

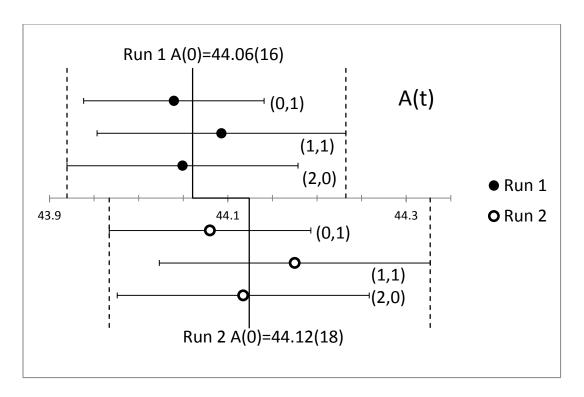| Fit, A(t) Run1	Parameters	Reduced χ2
Pade01	$\dfrac{44.04(10)}{1 + 0.31(01)x}$	1.16
Pade20	$44.05(13) - 13.7(10)x + 3.5(1.2)x^2$	1.37
Pade11	$\dfrac{44.09(14) + 3.4(5.7)x}{1 + 0.41(16)x}$	1.27

Figure 4 shows the values of Ao for three different PA forms that are not excluded, as well as the A10 form which has been rejected due to a poor reduce χ2 value and outlier value compared to the other PAs. Run 1 is shown on top and run 2 below the center line, with the average value shown in a solid vertical line, and the extents of the uncertainty in the dotted vertical lines.

Similarly, analysis of PAs was carried out for the asymmetry vs. rate data, where the Geant4 simulation does not provide guidance regarding a preferred functional form. In this case, the (2,0), (1,1), and (0,2) forms were not excluded, with the higher order PAs failing the F-test and the (1,0) and (0,1) forms failing on the basis of poor reduced χ^2 values. Results of the $A(R)$ PA analysis are shown in table 2.

Table 2 shows the results of the Pade analysis for the fits of the A(R) data for Run 1 (top) and Run 2 (bottom) to the various forms $A_{n,m}$. For each PA, the intercept(with uncertainty), the F-test result and the reduced $\chi 2$ value are shown. PAs in red are excluded by the F-test while those in blue are excluded using the reduced $\chi 2$ value. PAs that will be considered are shown in bold type.

A(R),**Run1** Pade(n,m)	(0,m)	(1,m)	(2,m)	(3,m)
(n,0)		43.42(25),n/a,15.2	**43.98(10),84,1.3**	44.08(11),2.4,1.1
(n,1)	43.77(15),16.8,5.1	**44.08(09),90,1.3**	44.15(15),0.3,1.5	
(n,2)	**44.05(09),25.0,1.2**	44.04(12),-0.5,1.8	44.00(35),-0.9,1.9	
(n,3)	43.98(10),-1.23, 1.84			

A(R),**Run2** Pade(n,m)	(0,m)	(1,m)	(2,m)	(3,m)
(n,0)		43.47(28),n/a,12.6	**44.06(12),65,1.4**	44.20(12),3.6,1.02
(n,1)	43.81(19),12.1,5.3	**44.20(11),76,1.2**	44.00(17),-1.3,2.3	
(n,2)	**44.15(11),25,1.2**	44.34(24),0.5,1.4	43.96(84),-1.2,3.2	
(n,3)	44.06(13),-1.4,1.99			

Figure 5

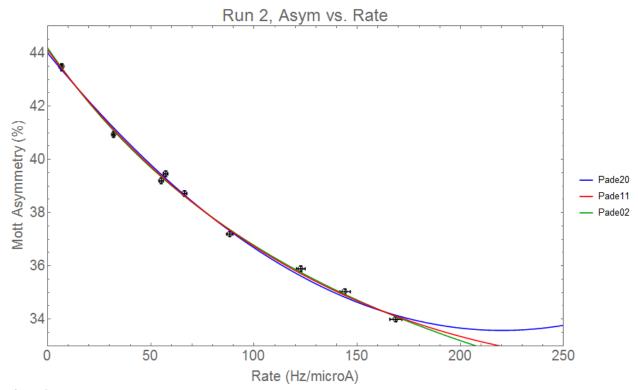| Fit, A(R) Run1	Parameters	Reduced χ2
Pade20	$43.95(10) - 0.087(3)x + 1.76(16)10^{-4}x^2$	3.01
Pade11	$\dfrac{44.07(10) + 0.0857(14)x}{1 + 4.19(42) \times 10^{-3}x}$	1.71
Pade02	$\dfrac{44.05(09)}{1 + 2.2(07) \times 10^{-3}x - 2.8(4) \times 10^{-6}x^2}$	2.00

Figure 6

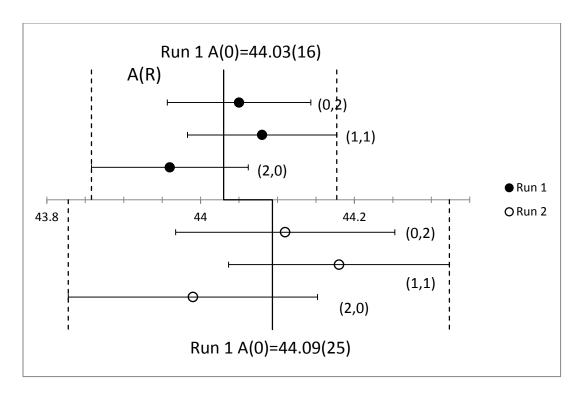| Fit, A(R) Run2	Parameters	Reduced χ2
Pade20	$43.99(16) - 0.0946(47)x$ $+ 2.15(26)10^{-4}x^2$	3.01
Pade11	$\dfrac{44.18(14) + 0.123(22)x}{1 + 5.36(68) \times 10^{-3}x}$	1.71
Pade02	$\dfrac{44.11(14)}{1 + 2.40(11) \times 10^{-3}x - 3.95(67) \times 10^{-6}x^2}$	2.00

Figure 7 shows the values of Ao for three different PA forms that are not excluded for the Rate vs. thickness data, as well as the A10 form which has been rejected due to a poor reduce χ^2 value and outlier value compared to the other PAs. Run 1 is shown on top and run 2 below the center line, with the average value shown in a solid vertical line, and the extents of the uncertainty in the dotted vertical lines.

.

This procedure was repeated once more for fits for the $R(t)$ data and the (1,0), (2,0) and (1,1) forms were not excluded, with results shown in table 3. Simulation for $R(t)$ suggests in this case that the (2,0) form is preferred for $R(t)$.

Table 3 shows the results of the Pade analysis for the fits of the R(t) data for Run 1 (top) and Run 2 (bottom) to the various forms $A_{n,m}$. The intercepts for all fits are forced through the point R(0)=0. For each PA, the F-test result and the reduced $\chi 2$ value are shown.

R(t),**Run1** Pade(n,m)	(1,m)	(2,m)	(3,m)
(n,0)	**n/a,2.7**	**17.2,0.89**	1.77,0.71
(n,1)	**14.0,1.13**	1.08,1.11	
(n,2)	0.76,1.18		

R(t),**Run2** Pade(n,m)	(1,m)	(2,m)	(3,m)
(n,0)	**n/a,3.4**	**21,0.98**	2.9,0.7
(n,1)	**18,1.2**	1.2,1.1	
(n,2)	1.1,1.2		

References

1. T.J. Gay and F.B. Dunning, "Mott Electron Polarimetry," Rev. Sci. Instrum. **63**, 1635 (1992).

2. Hodge et al. RSI 1979.

3. T.J. Gay, J.A. Brand, J.E. Furst, M.A. Khakoo, W.V. Meyer, W.M.K.P. Wijayaratna, and F.B. Dunning, "Extrapolation Procedures in Mott Electron Polarimetry," Rev. Sci. Instrum. **63**, 114 (1992).

4. G.D. Fletcher, T.J. Gay, and M.S. Lubell, "New Insights Into Mott–Scattering Electron Polarimetry," Phys. Rev. A **34**, 911 (1986).

4.1 J. Sromicki et al., "Polarization in Mott Scattering of Multi-MeV Electrons from Heavy Nuclei", Phys. Rev. Lett. 82, 57 (1999)

4.2 V. Tioukine, K. Aulenbacher and E. Riehn, "A Mott polarimeter operating at MeV electron beam energies", Rev. Sci. Instrum. 82, 033303 (2011)

4.3. H. Wegener, "Mott-Streuung an Streufolien endlicher Dicke", Zeitschrift für Physik A Hadrons and Nuclei 151, 252 (also reference Steigerwald conference proceedings)

4.4 M. Steigerwald, "MeV Mott Polarimetry at Jefferson Lab", AIP Conf. Proc. 570, 935 (2001)

5. J.Kallrath "Rational Function Techniques and Padé Approximants", in: Hagel, J. (Ed.), *Nonlinear Perturbation Methods with Emphasis to Celestial Mechanics* pp 97-107, Madeira University Press, Madeira, Portugal

6. Bevington, 2nd ed.

7. Ladish?

8. Measurements made using a Hitachi s-4700 FESEM with 15.0 kV electron energy.

9. Lebow Company, 5960 Mandarin Ave., Goleta, CA 93117, USA, lebowcompany.com

10. Brun, R. & Rademakers, F. (1996). ROOT - An Object Oriented Data Analysis Framework. AIHENP'96 Workshop, Lausane (p./pp. 81--86), .